Materials and Design 110 (2016) 519–525

Contents lists available at ScienceDirect

Materials and Design

journal homepage: www.elsevier.com/locate/matdes

Microstructural studies of oxide dispersion strengthened austenitic steels

Koppoju Suresh *, M. Nagini, R. Vijay, M. Ramakrishna, Ravi.C. Gundakaram, A.V. Reddy, G. Sundararajan

International Advanced Research Centre for Powder Metallurgy and New Materials (ARCI), Balapur PO, Hyderabad 500 005, Telengana, India

HIGHLIGHTS

- Designed a new ODS austenitic alloy composition to suppress the detrimental (delta and sigma) phases
- Synthesized the alloy through powder metallurgical process and has the hardness of 340 HV.
- Ultra-fine grain structure and even distribution of dispersoids (9 nm) in the alloy the observed to enhance hardness.

GRAPHICAL ABSTRACT

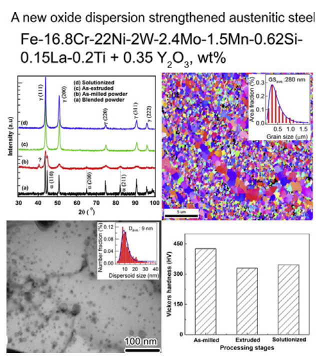

A new oxide dispersion strengthened austenitic steel Fe-16.8Cr-22Ni-2W-2.4Mo-1.5Mn-0.62Si-0.15La-0.2Ti + 0.35Y_2O_3, wt%.

ARTICLE INFO

Article history:
Received 28 April 2016
Received in revised form 3 August 2016
Accepted 5 August 2016
Available online 06 August 2016

Keywords:
Austenite
Dispersoids size
Microstructure
Hardness

ABSTRACT

Oxide dispersion strengthened (ODS) austenitic steel (Fe-16.8Cr-22Ni-2W-2.4Mo-1.5Mn-0.62Si-0.15La-0.2Ti + 0.35Y_2O_3, wt%) was prepared by mechanical alloying and consolidated by hot extrusion followed by solutionization at 1150 °C for 1 h. The composition of this steel is designed to suppress the formation of deleterious delta (δ-) ferrite and sigma (σ-) FeCr phases, which reduces the life the materials. Various microscopic, spectroscopic and diffraction techniques were employed to study the hierarchical microstructural features of this alloy. X-ray diffraction studies confirm the austenitic phase and no traces of δ-ferrite phase were observed in as-extruded and solutionized conditions. The solutionized austenitic ODS steel exhibited ultra-fine grain structure having mean sizes of 280 ± 5 and 440 ± 9 nm in transverse and longitudinal sections of the bar, respectively. Evenly dispersed high density of Y-Ti-O nano-oxides with a mean size of 9 nm was achieved along with low fractions of TiC and La rich $Y_2Si_2O_7$. The crystal structure of Y-Ti-O nano-oxides was determined by combining HR-TEM and FFT techniques and was found to be pyrochlore $Y_2Ti_2O_7$. These dispersoids and ultra-fine grain structure of austenitic steel contribute to an enhanced hardness of 346 ± 25 HV.

1. Introduction

Austenitic stainless steels possess good corrosion and oxidation resistance at elevated temperatures and are, therefore, used for many high temperature applications upto about 600 °C. The major limitation of Fe-based austenitic steels is their low yield strength and poor creep rupture strength as compared to Ni-based superalloys above 600 °C [1]. Although, high strength materials like precipitation hardened stainless steels are developed essentially for use in land/natural gas turbines, their use is limited to about 600 °C because of the growth of precipitates at temperatures beyond 600 °C [2]. Oxide dispersion strengthened (ODS) austenitic steels, in view of the stability of fine oxide dispersoids, should be lucrative alternatives to nickel base superalloys for use in hot sections of various turbines like casings, last stages of compressor blades, and various fasteners. The relatively better resistance of ODS

* Corresponding author.
E-mail address: sureshkoppoju@arci.res.in (K. Suresh).

http://dx.doi.org/10.1016/j.matdes.2016.08.020

austenitic steels at high temperatures even in marine environments can be gainfully used in marine gas turbines.

Processing of ODS steel involves mechanical alloying of elemental/pre-alloy powder of the desired steel composition with nano-Y_2O_3 particles, followed by consolidation of the powder either by hot extrusion or hot isostatic pressing. Since sufficient progress and understanding have already been achieved in fabrication of ferritic/martensitic and ferritic ODS steels with a controlled microstructure, a similar strategy can be applied to synthesize austenitic ODS steels. Recently, Kim et al. reported synthesis of austenitic ODS steel with composition close to AISI 316L through powder metallurgical process and obtained an ultimate tensile strength of 660 MPa at room temperature [3]. However, dispersoids of Y-Ti-O based complex oxides were not found. Instead, $Y_2Si_2O_7$ and TiO_2 particles with a size of few hundreds of nanometers were reported to be present in the steel matrix. Zhou et al. also reported the presence of Y-Ti-Si-O complex oxides of 20 nm with an ultimate tensile strength of 1000 MPa in ODS austenite steels [4]. It is also reported that addition of Zr and Hf to PNC316 austenitic ODS steel further reduces the average size of the complex oxides down to 6 nm from 14 nm on annealing at 1200 °C [5]. These complex oxides exhibit faceted type morphology and an anion-deficient fluorite $Y_2Hf_2O_7$ type crystal structure [6]. Zhou et al. reported improved room temperature tensile strength (940 MPa) in HIPed austenite ODS steel having Y-Ti-Si oxide dispersoids of 17 nm when compared to base AISI304 austenite steel (300 MPa) [7, 8]. Incorporation of a high number density of nano-oxides in austenitic ODS steels enhances yield and ultimate tensile strength by almost 3 times even at temperatures beyond 700 °C [4,7]. However, austenitic ODS steels exhibit inferior ductility in a temperature range of 600–900 °C, which may be due to the formation of σ-phase (FeCr) that causes the brittleness [8]. During prolonged exposure to high temperatures, austenitic steels suffer from embrittlement due to nucleation of Cr-rich (α′), Fe-rich (α), ordered FeCr and Laves phases [9,10,11]. The presence of a very low fraction of the δ-ferrite, which co-exists also causes the embrittlement [12]. These detrimental phases can be suppressed in the austenite steel by choosing the right combination of chromium equivalent (Cr_{eq}) and nickel equivalent (Ni_{eq}) for δ-ferrite phase [13, 14,15] and electron vacancy number ($\overline{N}_v$) for the σ-phase [16,17]. Woodyatt et al. developed an empirical relation to estimate the $\overline{N}_v$ from the composition of the alloy [16]. If the $\overline{N}_v$ is higher than 2.52, the σ-phase precipitates in the alloy, with the propensity of precipitation increasing with increase of $\overline{N}_v$. Table 1 summarizes the reported austenitic ODS steel compositions along with calculated Cr_{eq}, Ni_{eq} and $\overline{N}_v$ values in addition to results from mechanical properties. The $\overline{N}_v$ value of each of the alloys studied is much higher than 2.52, which indicates that the appearance of σ-phase is inevitable in these austenitic ODS steels [4–8,18,19]. Moreover, the Cr_{eq} and Ni_{eq} values indicate that the reported alloys are not completely in the austenite phase field [3–8,18].

In this study, the alloy composition was carefully designed such that the alloy is completely in austenitic phase field without the formation of δ-ferrite, while suppressing the tendency to form σ-phase under prolonged exposures at high temperatures. Therefore, the nominal chemical composition of the austenitic steel selected for the present study is Fe-16.8Cr-22Ni-2W-2.4Mo-1.5Mn-0.62Si-0.15La-0.2Ti (wt%), where Ni and Mn stabilize the austenitic phase and Cr improves resistance to corrosion and oxidation. Addition of La further enhances high temperature oxidation resistance by forming a thin layer of La rich chromium oxide below the chromia scale (surface Cr_2O_3 layer), thereby preventing further sublimation of the Cr [20]. W and Mo contribute to solid solution strengthening [21]. In the presence of Ni and Cr, Mo improves resistance to pitting corrosion [22,23]. A small fraction of Ti in this alloy greatly helps to reduce the size of the complex and stable Y-Ti-O based oxides [24]. The alloy was designed such that primary strengthening is due to oxide dispersoids (5–10 nm) and not with the carbides and the nitrides of MX type. The present paper discusses the development of microstructure of the matrix and the structure of dispersoids in ODS austenitic steel.

2. Experimental

The ODS austenitic steel with composition of Fe-16.8Cr-22Ni-2W-2.4Mo-1.5Mn-0.62Si-0.15La-0.2Ti + 0.35Y_2O_3, wt% was prepared by mechanical alloying, followed by hot extrusion. Austenitic SS316L alloy powder was prepared by water atomization technique. To attain the proposed composition of the alloy, Ni, Cr, W, Ti, NiLa powder were added to the SS316L powder and the mixture was blended along with Y_2O_3 powder and mechanically milled in Zoz Simoloyer CM-08 mill at 700 rpm for 4 h with a ball to powder ratio of 10:1 using SS vial and

Table 1

Summary of the compositions, mechanical properties and other structural data in comparison with the reference data.

Composition (wt%)	N_v	Cr_{eq}/Ni_{eq}	Presence of δ, σ phase	Processing stages	Precipitates/oxide dispersoids (size, nm)	Mechanical property	Ref.
Fe-16.56Cr-11.23Ni-2.19Mo-0.12Mn-0.81Si-0.029C-0.30Ti + 0.35Y_2O_3	2.76	21.86/12.16	δ, σ	HIPed @ 1150 °C	TiO_2 (~300) $Y_2Si_2O_7$ (~400)	UTS 670 MPa	[3]
Fe-18Cr-8Ni-1Mo + 0.5Ti + 0.35Y_2O_3	2.89	20.25/8.0	δ, σ	HIPed @ 1100 °C	Y-Ti-Si-O (~20) TiN (>100)	UTS 1000 MPa YS 960 MPa	[4]
Fe-16.16Cr-13.66Ni-2.33Mo-1.82Mn-0.18Ti-0.75Si-0.08Nb-0.05C-0.5Zr + 0.35Y_2O_3	2.68	21.97/16.07	δ, σ	Powder annealed @ 400–1200 °C	$Y_2Hf_2O_7$ (~5.9) $Y_2Zr_2O_7$ (~6.0)		[5]
Fe-16.16Cr-13.66Ni-2.33Mo-1.82Mn-0.18Ti-0.75Si-0.08Nb-0.05C + 0.6Hf + 0.35Y_2O_3	2.67	22.29/16.07	δ, σ	Hot extrusion @ 1100 °C	$Y_2Hf_2O_7$ (~10)		[6]
Fe-18Cr-8Ni-2W-1 Ti-0.35Y_2O_3	2.86	21.0/8.0	δ, σ	HIPed @ 1150 °C	Y-Ti-O (10–80)	UTS 775 MPa	[7]
Fe-18Cr-8Ni-1Mo + 0.5Ti + 0.35Y_2O_3	2.89	20.25/8.0	δ, σ	HIPed @ 1100 °C	TiN (large) Y-Ti-O (fine ~17)	UTS 940 MPa	[8]
Fe-20Ni-14Cr-2.5Mo-2.5 Al-2Mn + 0.5 & 5% Y_2O_3	2.64	31.5/21.0	δ, σ	Powder annealed and hot pressing @ 1150 °C	$YAlO_3$, Y_2O_3, Al_2O_3, $Y_2Al_5O_{12}$		[18]
Fe-24.5Cr-19.2Ni-0.46Ti-0.44N-0.019C-0.22Y-0.2O (ex.)	2.92	25.19/30.77	σ	HIPed @ 1100 °C	Y-Ti-O (10 − 20)	UTS 904 MPa	[19]
Fe-16.8Cr-22Ni-2W-2.4Mo-1.5Mn-0.62Si-0.15La-0.022C-0.2Ti + 0.35Y_2O_3	2.54	23.44/23.41	–	Hot extrusion @ 1150 °C	$Y_2Si_2O_7$ (~100) TiC (~40) $Y_2Ti_2O_7$ (~9)	VH 346 ± 20 HV	Present work